



Feeding-induced plant metabolite responses to a phoretic gall mite, its carrier psyllid and both, after detachment

Mengke Yang¹ · Jianling Li^{1,2} · Haili Qiao¹ · Kun Guo¹ · Rong Xu¹ · Hongshuang Wei¹ · Jianhe Wei¹ · Sai Liu¹ · Changqing Xu¹

Received: 8 February 2023 / Accepted: 10 October 2023 / Published online: 26 October 2023
© The Author(s), under exclusive licence to Springer Nature Switzerland AG 2023

Abstract

Phoresy is one of the most distinctive relationships between mites and insects, and the off-host interaction between phoretic mites and their carriers is the most critical factor sustaining the phoretic association. As phoretic associations commonly occur in temporary habitats, little is known about off-host interactions between phoronts and carriers. However, an off-host interaction has been reported, in which the plant-mediated competition between a phoretic gall mite, *Aceria pallida*, and its psyllid vector, *Bactericera gobica*, after detachment decreases leaf abscission caused by *B. gobica* and then directly facilitates their phoretic association. In this obligate phoresy, *A. pallida* seasonally attaches to *B. gobica* for overwinter survival and they share the same host plant, *Lycium barbarum*, during the growing season. It is unknown how the host plant responds to these two herbivores and what plant metabolites are involved in their interspecific interaction. Here, effects of *A. pallida* and *B. gobica* on the host plant's transcriptome and metabolome, and on enzymes involved in plant defence, at various infestation stages were studied by inoculating *A. pallida* and *B. gobica* either separately or simultaneously on leaves of *L. barbarum*. Our results showed that (a) *A. pallida* significantly promoted primary and secondary metabolite accumulation, (b) *B. gobica* markedly inhibited primary and secondary metabolite accumulation and had little influence on defence enzyme activity, and (c) under simultaneous *A. pallida* and *B. gobica* infestation, an intermediate response was predicted. These findings indicate that *A. pallida* and *B. gobica* have different effects on host plants, *A. pallida* inhibits *B. gobica* mainly by increasing the secondary metabolism of *L. barbarum*, whereas *B. gobica* inhibits *A. pallida* mainly by decreasing the primary metabolism of *L. barbarum*. In conjunction with our previous research, we speculate that this trade-off in host plant metabolite response between *A. pallida* and *B. gobica* after detachment promotes a stable phoretic association.

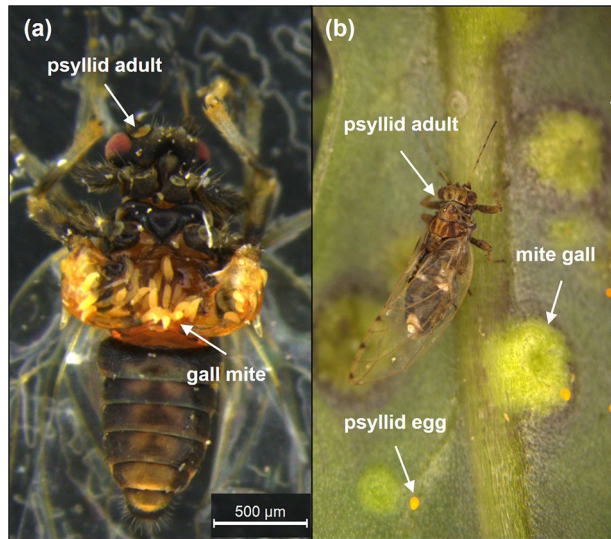
Keywords Phoresy · Gall mite · Psyllid · Interspecific competition · Metabolite communication

Introduction

Mites and insects show a great variety and unique types of associations, such as predation, parasitism, commensalism, and phoresy (Sarangi et al. 2010). Phoresy is an interaction in which one organism (the phoront) gains an ecological or evolutionary advantage by migrating from the natal habitat while superficially attached to a selected heterospecific host (the dispersal host) for some portion of the individual phoretic's lifetime; phoresy has been widely regarded as a form of coevolution or coadaptation (Binns 1982; White et al. 2017). Mites do not have wings, and most of them are restricted in dispersal, exhibiting clumsy and slow movement and the inability to cover large distances, so they depend on other animals for long-distance migration (Binns 1982). Mites have long engaged in phoresy, which generally comprises three distinct stages: locating a dispersal host, attaching to the host, and detaching from the host (Binns 1982). Traditionally, research on phoretic interactions has mainly focused on host location and attachment stages; research on the former explains how phoronts find hosts (via chemical cues such as long-chain fatty acid ethyl esters and CO₂), and research on the latter explains how phoronts stay on the host (via physical structures such as the pedicel and chelicera) and affect the host (protecting their hosts from parasites) (Bartlow and Agosta 2021). Only a few studies have focused on the detachment stage to identify the factors that determine disengagement of the phoront from the host, for example, humidity has been shown to be a factor for phoront's detachment from their vectors – these results have been promising for further study (Behura 1956; Okumura et al. 2013). As phoresy is a temporary form of symbiosis, the off-host interactions between phoronts and their carriers likely play an important role in sustaining the phoretic association (Seeman and Walter 2022). However, because most phoretic mites occur in temporary habitats such as dung, carrion, fungi, or plant debris (Binns 1982; Perotti and Braig 2009), little is known about what happens after detachment. Most study systems have been based on feeding or a limited number of observations; nevertheless, these systems have rarely been studied, and a more stable and common phoretic system is needed to study off-host interactions (Seeman and Walter 2022).

Liu et al. (2016) reported a seasonal phoretic association between the herbivorous gall mite *Aceria pallida* Keifer (Acari: Eriophyidae) and *Bactericera gobica* Loginova (Hemiptera: Psyllidae) from the same host plant, *Lycium barbarum* L. (also called wolfberry or goji). The gall mite intentionally enters the cavity between the hindleg coxae of the psyllid to escape unfavourable winter conditions and returns to the buds of the host plant early in the following spring (Fig. 1a). Subsequently, Li et al. (2018) demonstrated that *A. pallida* and *B. gobica* compete with each other after detachment and mixed infestation decreases the leaf abscission caused by the psyllid, which promotes the persistence of the psyllid population and indirectly facilitates the maintenance of the phoretic association. The detached gall mite and its vector feed on the same foliage, wherein the former infests the leaf tissues, induces galls, and resides and reproduces within the gall, and the latter lays eggs on the same leaves (Fig. 1b). Therefore, they are likely to be competitors for resources and habitat during the growing season (see also Wu et al. 2022). Nevertheless, a benefit might be associated in this interaction facilitating the trade-off between them in the long term. How the phoretic mite *A. pallida* and its vector *B. gobica* manipulate the host plant *L. barbarum* to interact with each other and the mechanism underlying this process are still unclear.

Fig. 1 The gall mite *Aceria pal-lida* and its vector *Bactericera gobica*. **a** Phoretic mites in the cavity between the hindleg coxae of the psyllid for overwintering. **b** Psyllid and gall mite on a same leaf of *Lycium barbarum* during the off-host period



Interspecific interactions among herbivores often occur when different species of arthropods exploit the same limited resources (Kessler and Baldwin 2004). Such interactions can be either negative or positive, but most of them are competitive, whereas fewer are facilitative (Kaplan and Denno 2007). Interspecific competition is often asymmetrical, that is, the effect of one species on another can be much stronger than the reverse (Wu et al. 2014). Psyllids often influence the health of host plants, as phloem-feeding insects, they compete with other herbivores by consuming nutrients from host plants and inducing plant defences (Harrison et al. 2021). For example, the Asian citrus psyllid, *Diaphorina citri* Kuwayama (Hemiptera: Psyllidae), can reduce the amino acid content of the host plant (Chin et al. 2017). Eriophyoid mites are obligatory plant feeders with unusual morphological, biological, and behavioural specializations compared to other mites, particularly gall-making species (Skoracka et al. 2009). Most gall-making mites are host specific, sharing an intimate relationship with host plants because of their ability to induce gall formation and spend most of their lifetime within galls (de Lillo et al. 2018). The biochemical cross-talk between gall inducers and host plants indicates that gall inducers have the best ways for deviating from plant chemical and defensive counterattack (Coelho Kuster et al. 2020). Compared with free-living herbivores, gall makers are likely to be more effective at manipulating the structure and metabolism of host plants, such as by regulating the levels of nutrients and secondary metabolites (Inbar et al. 2004; Hirano et al. 2020). For example, a significant increase in the level of total phenols was observed in galls induced by the gall mite *Aceria pongamiae* Keifer (Nasareen et al. 2012). Therefore, gall makers are likely to be superior competitors when competing with other herbivores (Prior and Hellmann 2010; Rostas et al. 2013). For example, the gall midge *Rabdophaga rigidae* Osten Sacken (Diptera: Cecidomyiidae) could enhance nutrient resources for other herbivores feeding on the same host plant; additionally, the gall wasp *Neuroterus saltatorius* Edwards (Hymenoptera: Cynipidae) could inhibit the performance of a butterfly caterpillar sharing the same plant (Nakamura et al. 2003; Prior and Hellmann 2010).

Plants employ various strategies to defend themselves against herbivores – plant primary metabolites as well as secondary metabolites play crucial roles in plant growth and development and reduce the threat of injury and loss of productivity (Fürstenberg-Hägg et al. 2013). Identifying the defensive traits expressed by plants to deter herbivores or limit herbivore-mediated damage and understanding the underlying defence mechanisms are crucial for understanding plant-herbivore interactions (Mitchell et al. 2016). A holistic view of plant primary/secondary metabolism and the multiple hormonal signal pathways that modulate these changes is required for understanding how plants shape interactions among herbivores that share a host (Lee et al. 2017). Both transcriptomics and metabolomics may be performed to explore the overall changes in organisms under specific conditions, revealing the changes in gene expression and metabolites, respectively, in plants responding to biotic and abiotic stress (Mutwakil et al. 2017; Chen et al. 2018). The purpose of the present work was to reveal the mechanism and material basis of the process by which plant-mediated competition facilitates the phoretic association between a gall mite and its vector after detachment. This study was performed by identifying the transcriptomic, metabolomic, and biochemical responses of the host plant *L. barbarum* to infestation by *A. pallida* and *B. gobica*, both separately and simultaneously.

Materials and methods

Cultivated plant material

The study was conducted at the Institute of Medicinal Plant Development (IMPLAD), Chinese Academy of Medical Sciences & Peking Union Medical College (CAMS & PUMC), in Haidian District (40°2'N, 116°16'E), Beijing, China. Seeds were collected in 2018 from wolfberry (*L. barbarum*) fruit (cultivar Ningqi No. 1) from Zhongning County (37°29'N, 105°42'E), Ningxia Hui Autonomous Region, China. The seeds were sown in plastic trays (54×28×11 cm) containing potting soil medium (muck soil, Meihokou, Jilin, China) for germination and cultivated in growth chambers (PGX-450 C, Saifu, Zhejiang, China) under the following conditions: 25±2 °C, 60±5% relative humidity (RH), L14:D10 photoperiod, and 18,000 lx illumination. Approximately 6 weeks after sowing, every seedling with approximately 10 leaves was transplanted into a plastic cup (6.5×6.5×9 cm) and watered once every 3 days for continued cultivation under the abovementioned conditions. No fertilization was applied during germination and cultivation. Approximately 2 weeks after transplantation, uniform seedlings with ca. 15–20 leaves were selected for subsequent experiments.

Herbivore resources and infestation

The specimens of *A. pallida* and *B. gobica* used in the laboratory were originally collected from the wolfberry experimental field located at IMPLAD and then reared separately on wolfberry seedlings for more than 30 and 10 generations, respectively, in growth chambers under the abovementioned conditions. Four treatments were performed: control (CK group), mite infestation (M group), psyllid infestation (P group), and mite+psyllid infestation (MP group) (Fig. 2). The infestation method used has been described previously (Li et

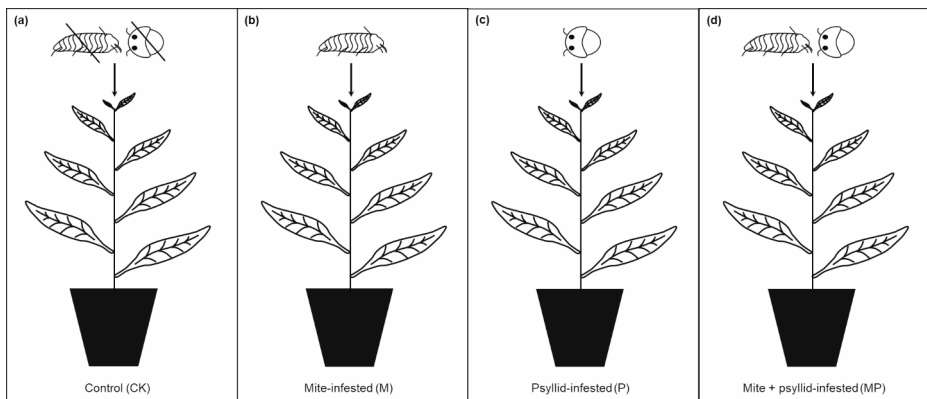


Fig. 2 Experimental design for the four treatments in the present study. **a** CK (control) group, not inoculated with herbivores. **b** M group, inoculated with ca. 30–50 gall mites. **c** P group, inoculated with ca. 50–60 psyllids. **d** MP group, inoculated with both ca. 30–50 gall mites and 50–60 psyllids

al. 2018). For M group, mature *A. pallida* galls (approx. 3 mm in diameter) cultured in the chamber were cut into slices of 2×0.5 mm (30–50 adult mites in each slice) under a stereomicroscope (Leica EZ4, Leica Microsystems, Wetzlar, Germany), and then one slice was carefully attached to the tip of seedlings in the mite infestation treatment. Two days later, there were approximately 20–30 galls on each seedling, and the dry slices were removed. In order to prepare seedlings for the MP group, M group seedlings were prepared and 2 days after attaching cut slices with mite galls, 2–3 leaves with dozens of second- or third-instar psyllid nymphs were attached to the galled leaves; 24 h later, approx. 50–60 nymphs were retained on the galled leaves of each seedling, and the others were removed. Seedlings in the psyllid infestation treatment (P group) were inoculated with 50–60 psyllid nymphs, and the seedlings in the control treatment (CK group) were not inoculated with any herbivore. All the seedlings were cultivated under the abovementioned conditions.

Sample collection

Laboratory leaf samples were collected in October 2018 from the CK, M, P, and MP groups 6 days after psyllid infestation. Samples of 500 mg of leaves were collected per treatment for transcriptomic analysis with three replicates (10 seedlings each), and 1 g of leaves was collected per treatment for metabolomic analysis with three replicates (20 seedlings each). Leaf samples were also collected in the laboratory from the CK, M, P, and MP groups on days 3, 6, 9 and 12 after psyllid infestation – same time interval as in Li et al. (2018), most adult psyllids had reached adulthood and emerged approximately 12 days after psyllid infestation –, and 100 mg of leaves was collected per treatment for biochemical analysis with 3–5 replicates (6 seedlings each). Psyllid nymphs on the leaves were removed in advance, and then leaves were washed with water. Then, the leaves were harvested. Samples were flash-frozen in liquid N_2 and stored at -80 °C.

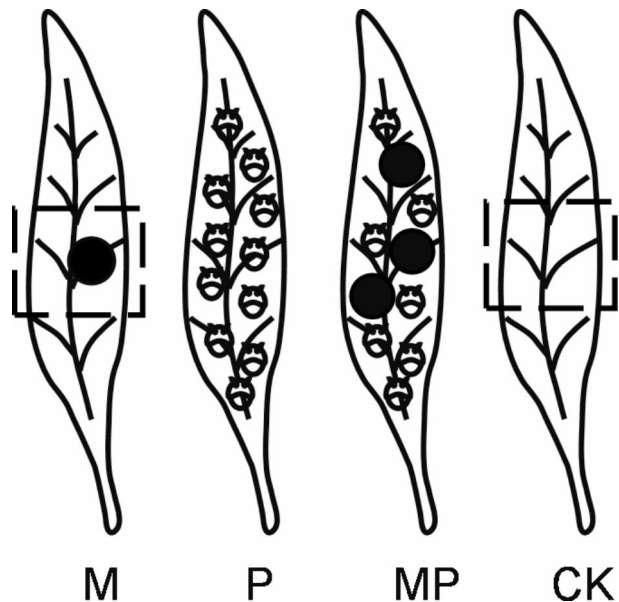
Field leaf samples were collected in May and July of 2019 at the IMPLAD wolfberry experimental field. The field treatments were similar with the previous study by Li et al. (2018), all pests and predators were cleared and infested with *A. pallida* or *B. gobica* using

the abovementioned method. Then, these trees were enclosed in cages (1×1×1.5 m, covered with white 80-mesh net) to limit the entrance of other pests. Clean leaves (based on inspection with the naked eye) were randomly selected in the field as non-infested leaves. Mite-infested leaves at three stages (stage I: 3–5 mm diameter, stage II: 5–7 mm diameter, stage III: >10 mm diameter), psyllid-infested leaves at three stages (stage I: instar 1–2, stage II: instar 3–4, stage III: instar 4–5) and mite+psyllid-infested leaves at one stage (gall diameter > 10 mm, instar 4–5 psyllid nymphs) were sampled as the treatment groups, and non-infested leaves from a similar position compared to the mite/psyllid-infested leaves from the same or adjacent non-infested branch were collected simultaneously as the control group. Sample preparation was performed as follows (Fig. 3): for mite-infested leaves from stages I–III, the dust was first cleaned from the surface. Then, taking the gall as the middle point, an approximately 1.0 cm² leaf area was cut off (labelled as M1, M2, M3). For psyllid- and mite+psyllid-infested leaves, the psyllid nymphs were removed first, and then the dust was cleaned off the leaf surface, taking the whole leaf samples as the treatment group (labelled as P1, P2, P3, MP). For non-infested leaves, sample preparation was performed as follows: the non-infested leaves were divided into three equal parts, and the middle part was retained as the control (labelled as CK1, CK2, CK3 and CK). A total of 1 g of leaves was collected per treatment for targeted determination with three replicates (10 plants each). All samples were flash-frozen in liquid N₂ and stored at -80 °C.

RNA extraction and transcriptome sequencing

Total RNA was isolated from frozen tissues using a TRIzol extraction kit (Tiangen Biotech, Beijing, China) following the manufacturer's instructions. RNA quality and quantity were determined by an Agilent Analyzer (2100 Bioanalyzer, Agilent Technologies, USA) and a NanoDrop spectrophotometer, respectively (ND2000, Thermo Fisher Scientific, DE,

Fig. 3 Field sample collection for the present study. **M** mite-infested leaves; **P** psyllid-infested leaves; **MP** mite+psyllid-infested leaves; **CK** control non-infested leaves



USA). High-quality RNA samples ($OD_{260}/_{280}=1.8\sim 2.2$, $OD_{260}/_{230}\geq 2.0$, $RIN\geq 6.5$, $28s:18s\geq 1.0$, $>10\ \mu\text{g}$) were used for subsequent analysis.

RNA-Seq and library construction were performed by Shanghai Biozeron Biotech (Shanghai, China) on the Illumina HiSeq 4000 platform. RNA-Seq transcriptome libraries were prepared by a TruSeq RNA Sample Preparation Kit from Illumina (San Diego, CA, USA) using $1\ \mu\text{g}$ of DNase-treated total RNA per sample. Briefly, mRNA was isolated with polyA selection by magnetic oligo (dT) beads and fragmented into small pieces using fragmentation buffer. cDNA synthesis, end repair, A base addition and ligation of the Illumina-indexed adaptors were performed according to Illumina's protocol. Libraries were then selected for cDNA target fragments of 200–300 bp on 2% Low Range Ultra Agarose, followed by PCR amplification for 15 cycles using Phusion DNA polymerase (NEB). After quantification by TBS380, paired-end libraries prepared for the CK, M, P, and MP groups were sequenced with an Illumina HiSeq PE 2×151 bp read length.

The raw paired-end reads were trimmed and quality controlled by Trinity (Eisen et al. 1998) and Tgici (de Hoon et al. 2004) software, respectively. The raw sequence data were publicly deposited in the National Centre for Biotechnology Information (NCBI) database under BioProject ID (PRJNA927104). A minimum total read count was applied for each tissue ($\text{min}=50$), and then differentially expressed genes (DEGs) among the four treatments were analysed. RNA-Seq data were normalized to fragments per kilobase of exon per million mapped reads (FPKM) values to quantify transcript expression. DEGs were identified by the following criteria: the absolute FPKM value was >10 , the fold change (FC) between treated group and control group was >2 (\log_2 ratio >1 or <-1) and $P<0.05$.

Metabolomic analysis

The freeze-dried samples were crushed using a mixer mill (MM 400, Retsch) for 1.5 min at 30 Hz. The 100 mg powder was weighed and extracted overnight at $4\ ^\circ\text{C}$ with 1.0 mL of 70% aqueous methanol. After centrifugation at 10 000 rpm for 10 min (SLM17, Thermo Scientific), the supernatant was filtered with a $0.22\ \mu\text{m}$ filter (ANPEL, Shanghai, China) before LC–MS/MS analysis. The quality control (QC) was prepared by mixing 20 μL of each of the above individual samples. The purpose of preparing QC samples was to test the reproducibility of the whole experiment.

The experiment was performed on a UPLC–ESI–MS/MS system (UPLC, ExionLC AD; MS, Applied Biosystems 6500 Triple Quadrupole). The samples were separated by using an ACQUITY UPLC HSS T3 C18 column ($100\ \text{mm}\times 2.1\ \text{mm}$, $1.8\ \mu\text{m}$, Waters Corporation, USA). The column temperature was $40\ ^\circ\text{C}$. The solvent system included ultrapure water with 0.04% acetic acid (A) and acetonitrile with 0.04% acetic acid (B). Compounds were separated using the following gradient program: 0–11 min, 95–5% A; 11–12 min, 5–5% A; 12–12.1 min, 5–95% A; 12.1–15 min, 95–95% A. The flow rate was $400\ \mu\text{L}\cdot\text{min}^{-1}$, and the injection volume was 2 μL .

The effluent was connected to an electrospray ionization (ESI)-triple quadrupole-linear ion trap (QTRAP)–MS.LIT and triple quadrupole (QQQ) scans were acquired on a triple quadrupole-linear ion trap mass spectrometer (QTRAP), AB Sciex QTRAP 6500 System equipped with an ESI-Turbo Ion-Spray interface, operating in both positive and negative ESI modes. The ESI source operation parameters were optimized as follows: the ion source was turbo spray; the source temperature was $500\ ^\circ\text{C}$; the ion spray voltage (IS) was 5,500 V

(positive) and $-4,500$ V (negative); and the curtain gas (CUR) was 25.0 psi. The collision-induced ionization parameter was set to medium. QQQ scans were acquired in multiple reaction monitoring (MRM) mode with optimized decluttering potential (DP) and collision energy (CE) for each individual MRM transition. The m/z range was set between 50 and 1,000. Data filtering, peak detection, alignment, and calculations were performed using Analyst v.1.6.1 software (AB Sciex). Metabolites were identified by searching the public databases: MassBank (<https://massbank.eu>), KNApSAcK (<http://www.knapsackfamily.com>), LIPDS MAPS (<https://www.lipidmaps.org>) and METLIN (<https://metlin.scripps.edu>) and comparing the m/z values, RT, and fragmentation patterns with those of the standards.

For statistical analysis, missing values were assumed to be below the limits of detection, and these values were input with a minimum compound value. The relative abundances of each metabolite were log-transformed before analysis to meet normality, and differential metabolites (DMs) among the four treatments were identified according to the following criterion: FC between treated group and control group was more than 2 (\log_2 ratio > 1 or < -1) and $P < 0.05$.

Biochemical analysis

Samples were powdered by a mixer mill (MM 400, Retsch) for 1.5 min (60 Hz, -20 °C). Then, the samples were analysed according to the instructions for assay kits for soluble sugars (Plant Soluble Sugar Content Test Kit A145-1-1), soluble proteins (Total Protein Quantitative Assay Kit A045-2-2), total phenols (Plant Total Phenol Test Kit A143-1-1), flavonoids (Plant Flavonoids Test Kit, A142-1-1), polyphenol oxidase (PPO) (Polyphenol Oxidase Test Kit, A136-1-1), peroxidase (POD) (Peroxidase Assay Kit, A084-3-1), and phenylalanine ammonia lyase (PAL) (Phenylalanine Ammonia Lyase Test Kit, A137-1-1). The concentrations of total C and N were determined by isotope analysis (Delta V Advantage, Thermo Fisher, USA). All kits used for biochemical analysis were purchased from Jiancheng Bioengineering Institute (Nanjing, China).

Determination of the targeted compounds

HPLC-grade acetonitrile (ACN) and methanol (MeOH) were purchased from Merck (Darmstadt, Germany). Milli-Q water (Millipore, Bradford, PA, USA) was used in all experiments. Acetic acid was purchased from Sinopharm Chemical Reagent (Shanghai, China). Scopoletin, ferulic acid and scoparone standards were purchased from Yuanye Bio-Technology (Shanghai, China).

The freeze-dried samples were crushed using a mixer mill (MM 400, Retsch) for 1.5 min at 30 Hz. Fifty mg of dried powder were extracted with 600 μ L of 70% MeOH. The extract was vortexed for 5 min and allowed to stand for 1 min at room temperature. Both processes were repeated twice, and then the extract was refrigerated overnight at 4 °C. The supernatants were collected after centrifugation at 12,000 rpm for 5 min (SLM17, Thermo Scientific) and filtering with a 0.22 μ m filter (ANPEL). Then, 120 μ L samples of the supernatants were taken for further LC–MS/MS analysis. The R^2 values of the three calibration curves were all > 0.990 (0.99092, 0.99966, 0.99322).

Stock solutions of standards were prepared at a concentration of 1 mg·mL⁻¹ in MeOH and stored at -20 °C. The stock solutions were diluted with MeOH to prepare working solu-

tions before analysis. Mixed standard solutions of the three compounds mentioned above were prepared in 70% methanol at 0.2, 0.5, 1, 2, 5, 10, 20, 50, 100, 200, 500, 1,000 and 2,000 $\text{ng}\cdot\text{mL}^{-1}$. The standard curve was drawn with the standard concentration ($\text{ng}\cdot\text{mL}^{-1}$) as the abscissa and the standard peak area as the ordinate. The concentrations of the three targeted compounds were determined as $\text{ng}\cdot\text{g}^{-1}$ of dried sample weight and calculated by the following formula: Concentration of the targeted compound ($\text{ng}\cdot\text{g}^{-1}$)= $A\times B/1,000/C$, where A represents the value calculated by substituting the integral peak area of the compound into the standard curve ($\text{ng}\cdot\text{mL}^{-1}$), B represents the volume of solution used for resolution (μL), and C represents the weight of the sample. Determination of the concentration of each sample was performed in triplicate.

The experiment was performed on a UPLC–ESI–MS/MS system (UPLC, Exion LC™ AD; MS, Applied Biosystems 6500 Triple Quadrupole). The samples were separated by using an ACQUITY UPLC HSS T3 C18 column (100 mm \times 2.1 mm, 1.8 μm , Waters Corporation, USA). The column temperature was 40 °C. The solvent system included water with 0.04% acetic acid (A) and acetonitrile with 0.04% acetic acid (B). The gradient program was as follows: 0–1.5 min, 2% B; 1.5–6 min, 95% B; 6–8 min, 95% B; 8.1–11 min, 2% B. The flow rate was 350 $\mu\text{L}\cdot\text{min}^{-1}$, and the injection volume was 2 μL . A QTRAP 6500 System (AB Sciex) equipped with an ESI-Turbo Ion-Spray interface, operating in both positive and negative ESI modes, was used. The ESI source operation parameters were optimized as follows: the ion source was turbo spray, the source temperature was 550 °C, the IS was 5,500 V (positive) and –4,500 V (negative), and the CUR pressure was 35.0 psi. The collision-induced ionization parameter was set to medium. The DP and CE for individual MRM transitions were performed with further DP and CE optimization. All instruments were controlled by Analyst v.1.6 software (AB Sciex).

Statistical analysis

For preliminary identification of transcriptomic and metabolomic associations between different groups of samples based on the similarity of their mass abundance profiles, hierarchical cluster analysis (HCA) was performed with TBtools software (<https://github.com/CJ-Chen/TBtools/releases>). For preliminary visualization of transcriptomic and metabolomic differences between groups of samples, the unsupervised dimensionality reduction method with partial least squares-discriminant analysis (PLS-DA) was performed with the SIMCA v.14.1 software package (Umetrics, Umeå, Sweden). All DEGs in the transcriptome were annotated and then placed into functional categories based on the software MapMan4 visualization toolkit (<https://mapman.gabipd.org>). IBM SPSS v.21.0 software for Windows (IBM, Armonk, NY, USA) was used to perform one-way ANOVA, followed by Duncan's multiple tests or Student's t test ($\alpha=0.05$).

Results

Integrated transcriptomic and metabolic analysis

Overview of the transcriptomic and metabolomics datasets

A total of 12 libraries (three biological replicates of four treatments) were examined, resulting in approximately 485,557 Mb of clean reads. After removing low-quality reads and reads with adaptor sequences, 163,694 unigenes were ultimately obtained in all samples, with a total length of 190,629,707 base pairs (bp) and an average length of 1,164 bp. The GC content accounted for 40.2%. Examination of the transcriptome revealed 4 390 DEGs among the four treatments. In total 2,003 DEGs were identified between the M and CK groups, of which 1,192 were upregulated and 811 were downregulated. A total of 2,490 DEGs was identified between the P and CK groups, of which 1,632 were upregulated and 858 were downregulated. A total of 3,522 DEGs was identified between the MP and CK groups, of which 2,198 were upregulated and 1,324 were downregulated (Fig. 4a). PLS-DA showed that transcripts from the four groups were separated, and the three biological replicates from each group clustered together. This indicated that the transcript profiles from each group were significantly different and highly reproducible. The difference between the CK and M groups was relatively small, as was that between the P and MP groups (Fig. 4b). The heatmap showed differences in the transcript data (three replicates for each group), which was consistent with the PLS-DA results (Fig. 4c).

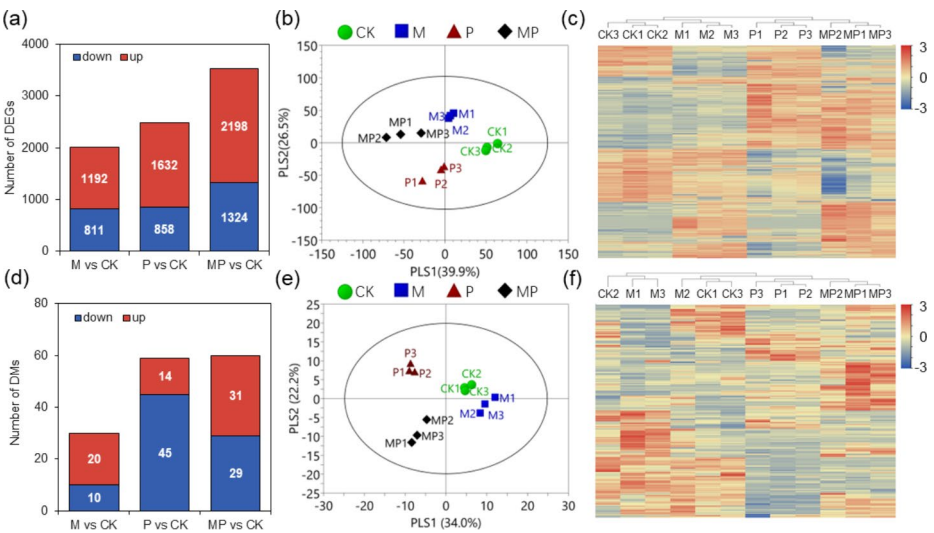


Fig. 4 Comparison of the transcriptomic and metabolomic profiles of *Lycium barbarum* leaves under the *Aceria pallida*, *Bactericera gobica* and *A. pallida*+*B. gobica* infestation treatments. **a** Number of differentially expressed genes (DEGs); **b** number of differential metabolites (DMs); **c** partial least squares-discriminant analysis (PLS-DA) of transcripts; **d** PLS-DA of metabolism; **e** heatmap of transcripts; **f** heatmap of metabolites. Red indicates upregulation and blue indicates downregulation in the bar chart and heatmap. Green denotes the control treatment (CK), blue denotes the mite-infested treatment (M), red denotes the psyllid-infested treatment (P) and black denotes the mite+psyllid-infested treatment (MP) in the PLS-DA diagram. The replicates are labelled 1, 2, and 3. Lines connect samples from the same treatment in the PLS-DA diagram

A total of 202 known compounds from 16 classes was detected in *L. barbarum* leaves by LC–MS/MS. 92 primary and 110 secondary metabolites were identified among the groups of samples. Examination of the metabolites revealed 96 DMs among the four treatments. 30 DMs were identified between the M and CK groups, of which 20 were upregulated and 10 were downregulated. 59 DMs were identified between the P and CK groups, of which 14 were upregulated and 45 were downregulated. 60 DMs were identified between the MP and CK groups, of which 31 were upregulated and 29 were downregulated (Fig. 4d). Consistent with the transcriptome data, both the PLS-DA and heatmap of the metabolome data showed that the differences between the CK and M groups and between the P and MP groups were relatively small (Fig. 4e and f). Based on a combination of the transcriptome and metabolome data, we concluded that compared to the gall mite *A. pallida*, which had a weak effect on wolfberry's transcripts and metabolites, the psyllid *B. gobica* had a strong effect, and the effect on wolfberry was compromised when the two herbivores fed together.

Metabolic pathway analysis of DEGs and DMs

In total, 2,762 DEGs were annotated into 50 functional categories of plants by MapMan4, mainly including photosynthesis, carbohydrate metabolism, and secondary metabolism.

In photosynthesis, analysis of the DEGs showed that compared with the CK treatment, psyllids (P) had a stronger negative influence by inhibiting the photosynthetic system (PSI & PSII) as well as the Calvin cycle. In contrast, the gall mite (M) had little influence on the photosynthetic system (PSI & PSII) but promoted the Calvin cycle, indicating that the gall mites may have indirectly promoted photosynthesis in the host plant (Fig. 5a).

In primary metabolism, analysis of the DEGs showed that compared with the CK treatment, psyllids (P) had little influence on carbohydrate biosynthesis (sucrose and starch) but a positive influence on carbohydrate degradation and lipid biosynthesis/degradation as well as amino acid biosynthesis/degradation (Fig. 5b). Moreover, analysis of the DMs showed a decrease in the relative abundance of primary metabolites (e.g., carbohydrates, lipids, and amino acids) in psyllid-infested leaves (P) (Fig. 5c). However, analysis of the DEGs showed that gall mites could stimulate carbohydrate biosynthesis (sucrose and starch) and amino acid biosynthesis but inhibit carbohydrate and lipid degradation (Fig. 5b); accordingly, analysis of the DMs showed an increase in the relative abundance of primary metabolites (e.g., carbohydrates, lipids, and amino acids) in mite-infested leaves (M) (Fig. 5c).

In secondary metabolism, analysis of the DEGs showed that compared with the CK treatment, psyllids (P) had a weak influence on the biosynthesis of terpenes (including the mevalonate (MVA) and 2-C-methyl-d-erythritol 4-phosphate (MEP) pathways) and phenolics (including the precursor *p*-coumaroyl-CoA) (Fig. 5b). Moreover, analysis of the DMs showed a decrease in the relative abundance of secondary metabolites (e.g., phenolics and organic acids) in psyllid-infested leaves (Fig. 5c). However, analysis of the DEGs showed that gall mites (M) could stimulate secondary metabolism biosynthesis (phenolics and terpenoids) (Fig. 5b), and analysis of the DMs correspondingly showed an increase in the relative abundance of secondary metabolites, especially phenolics, in mite-infested leaves (Fig. 5c). Interestingly, in the gall mite+psyllid treatment (MP), the influence on photosynthesis and primary and secondary metabolism in the host plant was intermediate compared with the effects of *B. gobica* and *A. pallida* feeding separately.

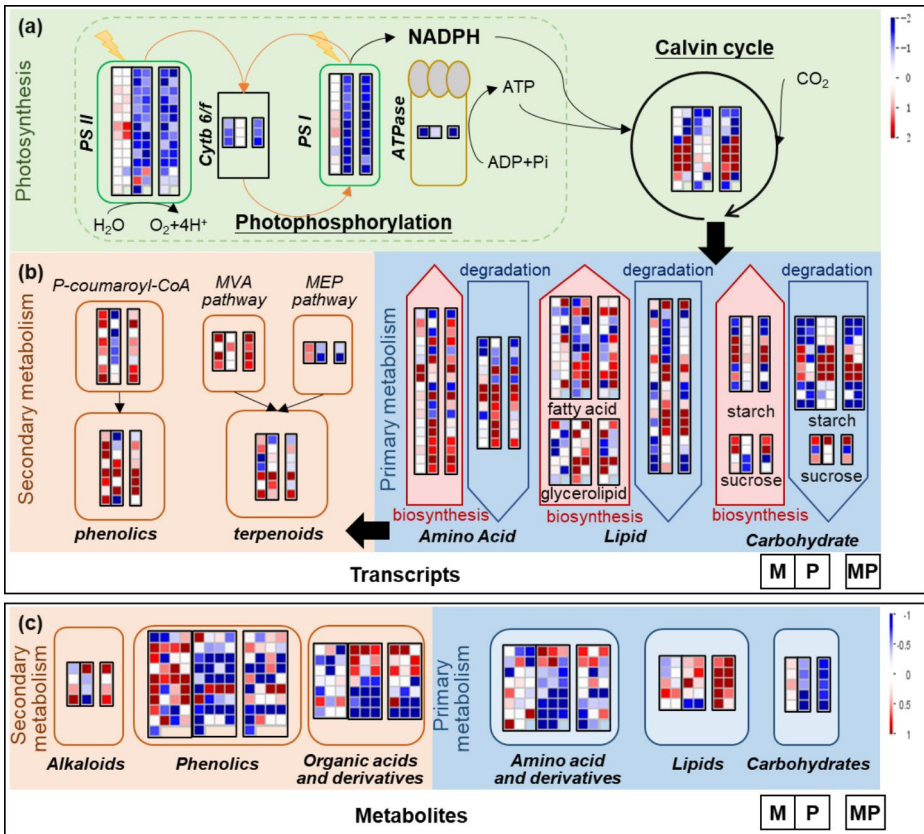


Fig. 5 Integrated annotation of transcriptomic and metabolic pathways in *Lycium barbarum* leaves under the *Aceria pallida*, *Bactericera gobica* and *A. pallida*+*B. gobica* treatments compared with the control treatment. **a** Photosynthetic pathway of transcripts; **b** primary and secondary metabolic pathways of transcripts; **c** primary and secondary metabolic pathway of metabolites. Each block from left to right corresponds to the mite-infested treatment (M), psyllid-infested treatment (P) and mite+psyllid-infested treatment (MP). Red denotes upregulation and blue denotes downregulation in the diagram

Biochemical analysis

Soluble sugar and soluble protein content

Sugar and protein are important nutrient resources for arthropods (Awmack and Leather 2002). The soluble sugar content was significantly higher in mite-infested leaves (M) at different times (3, 6, 9, 12 days) but showed a decreasing trend after psyllid infestation (P) and mite+psyllid infestation (MP) over time, significantly decreasing at 9 and 12 days (Fig. 6a). The soluble sugar content significantly increased after mite infestation (M) and decreased after psyllid infestation (P) whereas the mite+psyllid infestation (MP) was in between (Fig. 6b). The soluble protein content showed a gradually decreasing trend at 3 and 6 days after mite infestation (M) but did not significantly change at 9 and 12 days; it showed no significant difference over time after mite+psyllid infestation (MP) (Fig. 6c).

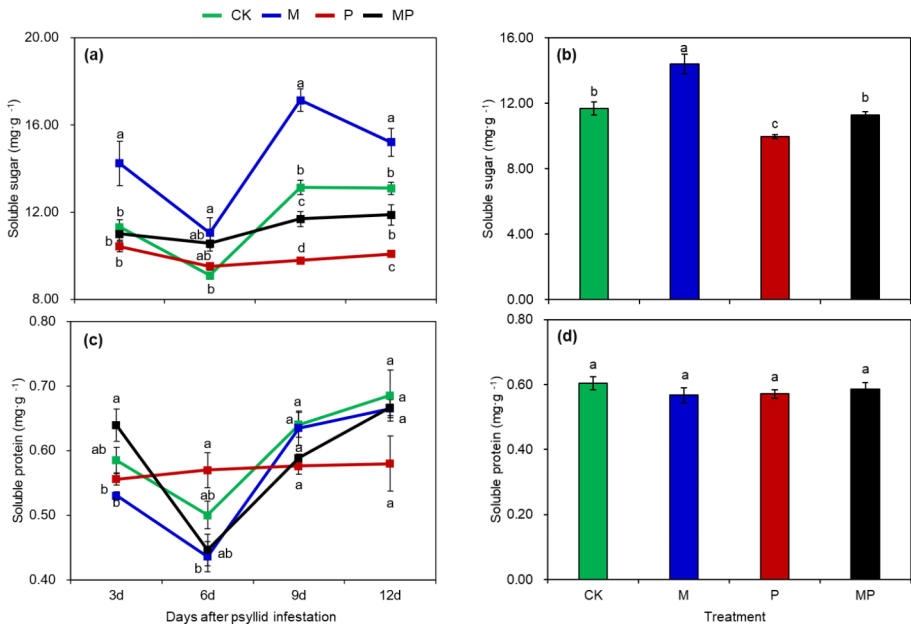


Fig. 6 Influence of the *Aceria pallida* and/or *Bactericera gobica* on mean (\pm SE, $n=3$) soluble sugar and soluble protein content ($\text{mg}\cdot\text{g}^{-1}$) of *Lycium barbarum*. **a** Dynamics of soluble sugar concentration at 3–12 days after psyllid infestation and **b** average of soluble sugar concentration under different treatments during mite and psyllid interaction; **c** dynamics of soluble protein concentration at 3–12 days after psyllid infestation and **d** average concentration of soluble sugar under different treatments during mite and psyllid interaction. The coloured lines and bars denote the control (CK, green), the mite infestation group (M, blue), the psyllid infestation group (P, red), and mite+psyllid infestation group (MP, black). Means within a panel marked with different letters are significantly different (Duncan’s multiple tests: $P<0.05$)

Soluble proteins were not significantly affected at any time when the two herbivores were both present (Fig. 6d).

Total carbon and total nitrogen content and C/N ratio

Plant carbon and nitrogen levels have long been linked to the performance and dynamics of arthropods (Mattson 1980). The carbon and nitrogen levels dramatically decreased in the psyllid-infested leaves (P) (Table 1). The carbon content in mite-infested leaves (M) was significantly lower than that in control leaves (CK), and their nitrogen content was the highest in all the treatments (Table 1). Therefore, the M leaves had the lowest C/N ratio, and the P leaves had the highest C/N ratio (Table 1). Thus, in the mite+psyllid-infested leaves (MP), the carbon and nitrogen content and C/N ratio were intermediate (Table 1).

POD, PPO and PAL activities

POD, PPO, and PAL are enzymes that are closely related to plant defence (Javadi Khederi et al. 2018). The activities of POD, PPO, and PAL increased initially and then decreased over time, peaking at 6 days in mite-infested (M) leaves (Fig. 7a, c and e) and they were generally significantly higher than those in the other treatments (Fig. 7b, d and f). The activities of

Table 1 Mean (\pm SE; $n=4$) C%, N%, and C/N ratio of *Lycium barbarum* leaves under the control (CK), *Aceria pallida* (M), *Bactericera gobica* (P) and *A. pallida*+*B. gobica* (MP) infestation treatments at 12 days after psyllid infestation

Group	C%	N%	C/N
CK	42.3 \pm 0.42 a	6.6 \pm 0.07 ab	6.4 \pm 0.08 b
M	40.6 \pm 0.13 b	6.8 \pm 0.09 a	5.9 \pm 0.07 c
P	37.5 \pm 0.47 c	5.5 \pm 0.04 c	6.8 \pm 0.10 a
MP	37.9 \pm 0.37 c	6.2 \pm 0.26 b	6.1 \pm 0.21 bc

Means within a column followed by different letters are significantly different (Duncan's multiple tests: $P<0.05$)

POD, PPO, and PAL in psyllid-infested leaves (P) showed no clear change with time on the whole (Fig. 7a, c and e) and they were generally not different from the control group (CK) (Fig. 7b, d and f). In mite+psyllid-infested leaves (MP), the POD, PPO and PAL activities also showed a trend of first increasing and then decreasing, peaking at 6 days (Fig. 7a, c and e); most of them showed intermediate activity values between those in M and P leaves (Fig. 7b, d and f).

Total phenol and total flavonoid levels

Phenolic compounds, including flavonoids, enable plants to adapt to changing biotic and abiotic stress in the environment (Cheynier et al. 2013). Our results showed that the levels of phenols and flavonoids had similar change trends under the different treatments. Total phenol and flavonoid concentrations in mite-infested leaves (M) showed first a decreasing and then an increasing trend (Fig. 8a and c); overall, gall mites could stimulate the accumulation of phenols and flavonoids in the host plant (Fig. 8b and d). Total phenol and flavonoid concentrations in psyllid-infested leaves (P) showed an increasing trend but were lower than the control treatment especially in the early stages (3, 6 days) (Fig. 8a and c), they were generally inhibited during the psyllid infestation (Fig. 8b and d). Total phenol and flavonoid levels in mite+psyllid-infested leaves (MP) were intermediate, especially at 9 and 12 days after infestation (Fig. 8a–d).

Determination of the levels of three phenolic compounds

To identify specific phenolic substances from total phenols during the off-host interaction, three differentially produced phenolic compounds (ferulic acid, scopoletin, and scoparone) were screened based on the metabolic profiles and were further examined. The results showed that the scopoletin content was the highest, followed by the ferulic acid and scoparone. Their concentrations in infested leaves were usually higher than in non-infested leaves (Fig. 9a–c).

The ferulic acid and scopoletin concentrations in mite-infested leaves (M) were significantly higher than those in the control group at all stages (Fig. 9a and b), whereas the scoparone concentration in M was dramatically higher than that in non-infested leaves (CK) at stage III only (Fig. 9c). The scopoletin and scoparone concentrations in psyllid-infested leaves (P) dramatically increased compared with those in CK leaves at stages I–II (Fig. 9b and c), whereas there was no difference in the ferulic acid concentration between P and CK leaves (Fig. 9a). Additionally, the ferulic acid and scopoletin concentrations in mite+psyllid-infested leaves (MP) were markedly higher than those in CK leaves (Fig. 9a and b), but no difference was detected in the scoparone concentration (Fig. 9c).

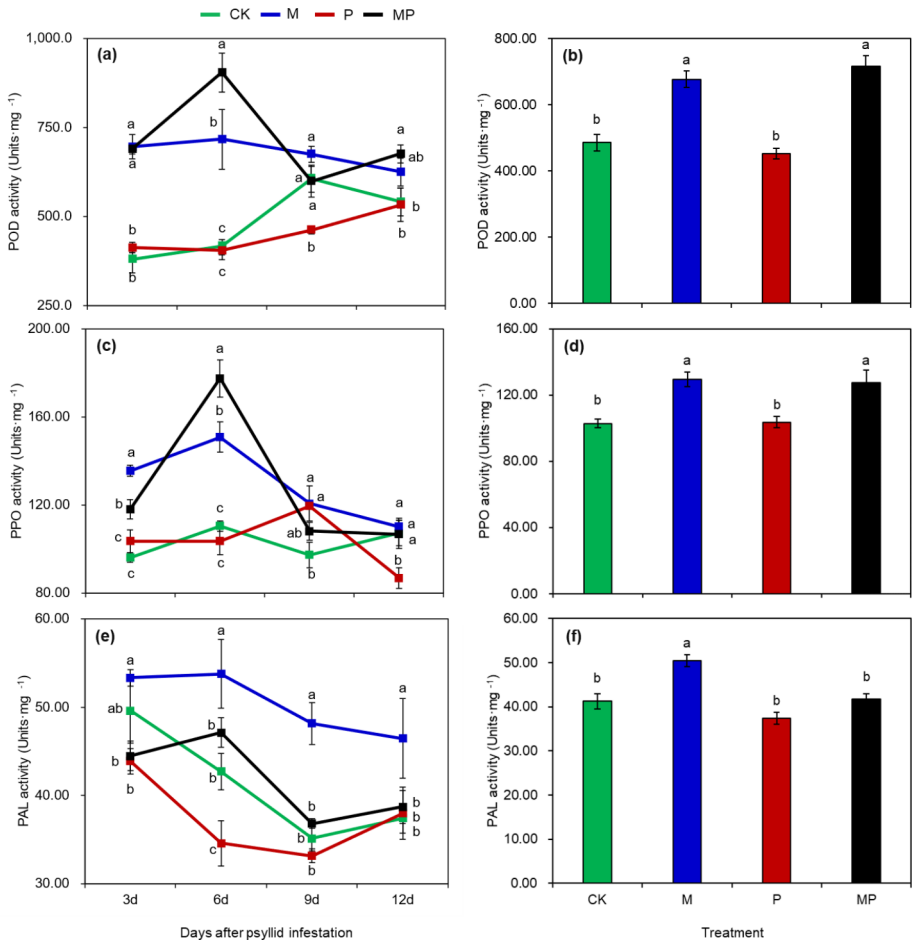


Fig. 7 Influence of *Aceria pallida* and/or *Bactericera gobica* on mean (\pm SE, $n=5$) peroxidase (POD), polyphenol oxidase (PPO) and phenylalanine ammonia lyase (PAL) activities ($\text{units}\cdot\text{mg}^{-1}$) of *Lycium barbarum*. **a** Dynamics of POD activity at 3–12 days after psyllid infestation and **b** average POD activity under different treatments during the mite and psyllid interaction; **c** dynamics of PPO activity at 3–12 days after psyllid infestation and **d** average PPO activity under different treatment during the mite and psyllid interaction; **e** dynamics of PAL activity at 3–12 days after psyllid infestation and **f** average PAL activity under different treatment during the mite and psyllid interaction. The coloured lines and bars denote the control (CK, green), the mite infestation group (M, blue), the psyllid infestation group (P, red), and mite+psyllid infestation group (MP, black). Means within a panel marked with different letters are significantly different (Duncan’s multiple tests: $P<0.05$)

Discussion

Our results showed that *A. pallida* had a weakly positive influence on photosynthesis of the host plant; it significantly promoted the accumulation of primary metabolites, such as carbohydrates, and it promoted defence responses, such as secondary metabolite accumulation and defence enzyme activity enhancement. *Bactericera gobica* had an obviously negative influence on photosynthesis in the host plant; it significantly promoted the degradation

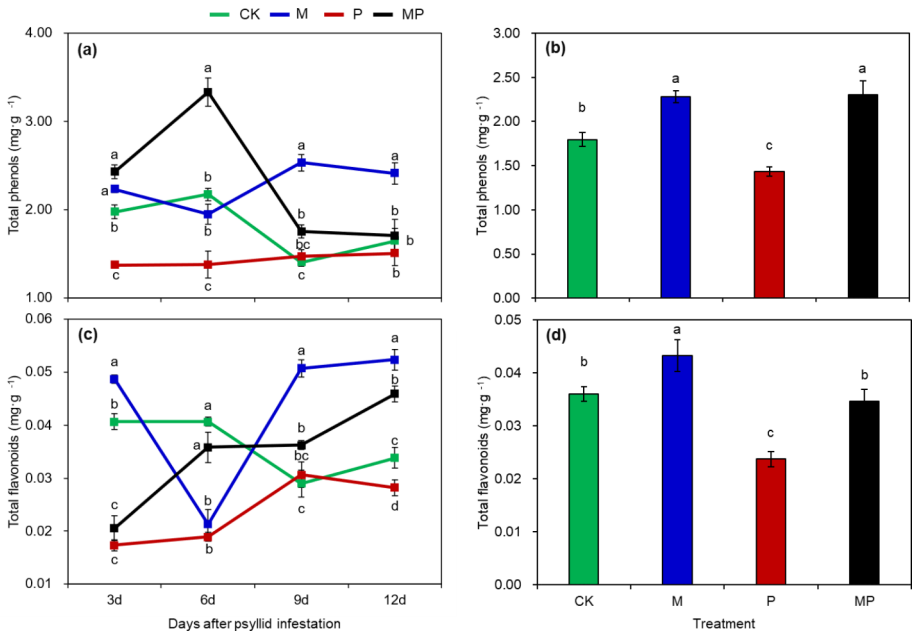
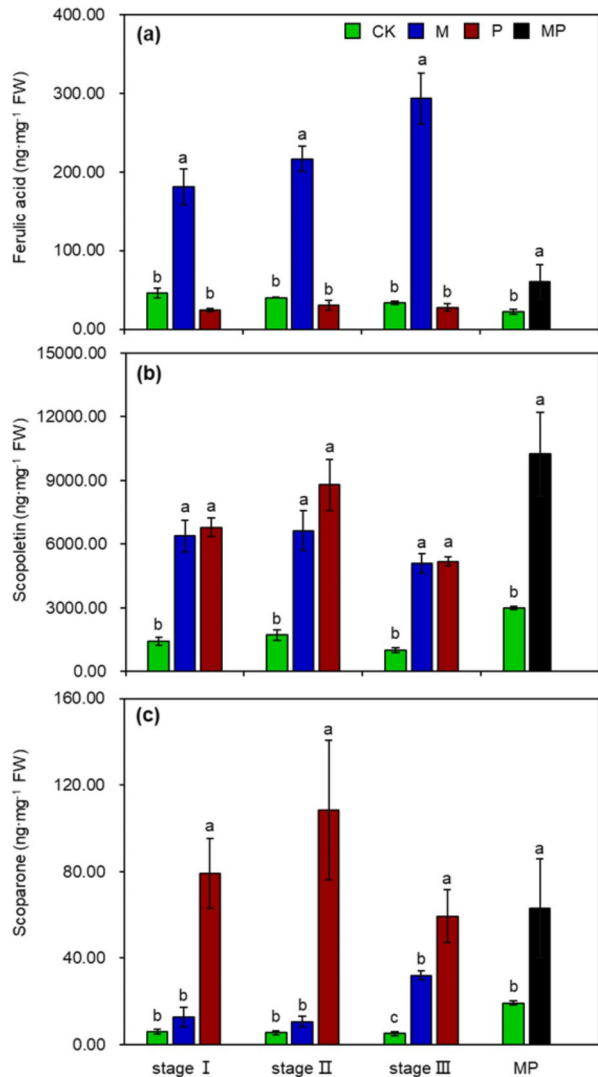


Fig. 8 Influence of *Aceria pallida* and/or *Bactericera gobica* on mean (\pm SE, $n=5$) total phenol and total flavonoid ($\text{mg}\cdot\text{g}^{-1}$) of *Lycium barbarum*. **a** Dynamics of total phenol concentration at 3–12 days after psyllid infestation and **b** average total phenols concentration under different treatments during the mite and psyllid interaction; dynamics of total flavonoid concentration at 3–12 days after psyllid infestation and **d** average total flavonoid concentration during the mite and psyllid interaction. The coloured lines and bars denote the control (CK, green), the mite infestation group (M, blue), the psyllid infestation group (P, red), and mite+psyllid infestation group (MP, black). Means within a panel marked with different letters are significantly different (Duncan's multiple tests: $P<0.05$)

of primary metabolites, such as carbohydrates and lipids, inhibited secondary metabolite accumulation and had a weak influence on defence enzyme activities. Under simultaneous feeding by *A. pallida* and *B. gobica*, an intermediate response including primary metabolites, secondary metabolites and defensive enzymes in wolfberry was predicted. Psyllids are sometimes called 'senescence-feeders' as they have evolved the capacity to accelerate the rate at which the tissues they feed on senesce, breaking down the chlorophyll and releasing nitrogen, thus enhancing the quantity and quality of their food (Morath et al. 2006; Steinbauer et al. 2014; White 2015). However, as the leaves continue to senesce, excessive depletion of carbohydrates and nitrogen usually induces foliar abscission (Addicott and Lynch 1955). For example, feeding by the melaleuca psyllid, *Boreioglycaspis melaleucae* Moore, accelerated foliar senescence increased the likelihood of leaf abscission by 4.7-fold compared with leaves not subjected to herbivory and was not influenced by leaf age or chemotype (Morath et al. 2006). Based on our previous work (Li et al. 2018), we speculate that *B. gobica* also accelerate foliar senescence and abscission, and the situation has mitigated in the presence of *A. pallida*. On the one hand, as a gall-inducer, *A. pallida* can increase the auxin content and alter source-sink relationships to gather more nutrients (Larson and Whitham 1991; Yang et al. 2023). On the other hand, enhanced secondary metabolites could inhibit excessive nutrient consumption by *B. gobica*. Meanwhile, the decrease of primary

Fig. 9 Influence of *Aceria pallida* and/or *Bactericera gobica* on mean (\pm SE, n=3) **a** ferulic acid, **b** scopoletin, and **c** scoparone concentration ($\text{ng}\cdot\text{mg}^{-1}$ fresh weight) in mite-infested leaves (M), psyllid-infested leaves (P) and mite- + psyllid-infested leaves (MP) of *Lycium barbarum* at different infestation stages (see Material and Methods)



metabolites induced by the psyllid could also partly inhibit the mite, and this trade-off mediated by the host plant would prevent excessive population growth of *B. gobica* or *A. pallida*, thus potentially achieving a delicate balance among host plant, psyllid and mite. Therefore, the host plant metabolite response to *A. pallida* and *B. gobica* could help understand the occurrence of the phoretic association. But additional experiments are needed to substantiate this assertion.

Photosynthesis is the main process involved in photosynthate accumulation and provides the precursor material of primary and secondary metabolites for plants (Paul and Foyer 2001). Photosynthesis was found to not be vital for the survival of gall inducers inside the gall, but the growth of shaded galls was substantially reduced (Haiden et al. 2012). Several studies have indicated that gall inducers may promote photosynthetic capacity through

increased water retention capacity (Fay et al. 1993) and CO₂ absorbance (Murakami et al. 2021) or even by inducing stomatal formation (Nabity et al. 2013) to compensate for increased carbon demand by galls (Dorchin et al. 2006). Therefore, we deduced from the RNA-Seq results that *A. pallida* promoted the photosynthesis-related Calvin cycle mainly through increased CO₂ absorbance. Psyllid species that feed on plants by ingesting phloem sap usually cause a decrease in chlorophyll and carotenoid levels in host plants (Othmen et al. 2022). For example, the tomato psyllid *Bactericera cockerelli* (Šulc) causes photosynthesis rate reduction in host plant leaves (Gao et al. 2016), and a subsequent study confirmed that psyllid infestation induces the downregulation of photosystem genes (Harrison et al. 2021). These studies strongly indicate that psyllid infestation could lead to impaired photosynthesis. Furthermore, there is evidence that *B. gobica* can inhibit root growth and leaf photosynthesis in *L. barbarum* significantly (Liu et al. 2020).

Gall inducers have a highly intimate nutritional relationship with their host plants because they spend a major portion of their lifetime within the gall (Florentine et al. 2005). Most gall inducers can manipulate primary and secondary metabolism in directly infested plant tissues, as well as tissues far from the feeding site (Stone and Schönrogge 2003; Petanovic and Kielkiewicz 2010). Nitrogen is crucial for the growth, development, and reproduction of herbivores (Awmack and Leather 2002), and higher N levels and a lower C/N ratio increase the feeding and/or fertility of herbivores (Meunier et al. 2016). The C/N ratio in *A. pallida*-infested leaves was lower than that in non-infested leaves, indicating the capacity of galls to serve as nutrient sinks, which was consistent with the ‘nutrient hypothesis’ (Stone and Schönrogge 2003). In addition, a previous study confirmed that the gall wasp *Leptocybe invasa* Fisher & La Salle (Hymenoptera: Eulophidae) induced a lower C/N ratio in galled leaves (Li et al. 2017). Galls play a role as nutrient sinks, thus helping gall inducers gain higher reproductive success (Inbar et al. 2004). However, phloem-feeding insects such as psyllids completely depend on the phloem nutrition of host plants. There are abundant sugars and low amounts of amino acids present in the phloem sap of most plants, so to fulfil their need for essential amino acids, phloem-sucking insects must consume a large amount of phloem sap (Byrne and Miller 1990; Hijaz et al. 2016); therefore, the soluble sugar content, C% and N% decreased significantly in *B. gobica*-infested leaves, and the higher C/N ratio in the *B. gobica*-infested leaves may be attributed to the psyllid’s great demand for amino acids. Our transcriptome and metabolome analysis also confirmed that *B. gobica* infestation caused significant consumption of primary metabolites.

As mentioned above, gall inducers spend a major portion of their lifetime inside the gall and cannot move freely like other unrestrained herbivores; therefore, the gall habitat is crucial to the survival of the gall inducer. As a result, gall inducers always enhance secondary metabolism in galls, especially the phenol production (Rehill and Schultz 2012; Kot et al. 2018), to defend themselves against other herbivores (Coelho Kuster et al. 2020) or microorganisms (Gerchman and Inbar 2011). Our results confirmed that the gall mite *A. pallida* significantly promoted the accumulation of secondary metabolites. PPO and POD are the two key enzymes that catalyse phenol oxidization, and PAL is a pivotal enzyme involved in phenolic biosynthesis (War et al. 2012; Cheynier et al. 2013), so these enzymes are linked closely to plant defence against biotic and abiotic stress. The levels of total phenols, total flavonoids and three phenolic compounds (ferulic acid, scopoletin and scoparone), as well as the activities of three defence-related enzymes (POD, PPO and PAL), all increased in the gall mite-infested leaves.

Plant responses to herbivores are strongly correlated with the mode of herbivore feeding and the degree of tissue damage at the feeding site (Walling 2000). The gall mite *A. pallida* and the psyllid *B. gobica* are both piercing-sucking arthropods, but psyllids are phloem-feeding herbivores, and gall mites are herbivores that feed on cellular contents (Walling 2000). Phloem-feeding herbivores, such as psyllids, aphids, and whiteflies, do not always trigger a defence response because they cause only minor tissue damage (Wang et al. 2017; Patton et al. 2018; Malka et al. 2020). However, gall mites that lacerate cells cause more extensive tissue damage and deformities, and thus, the response of plants to these mites is more similar to their response to chewing herbivores (Walling 2000). Our results also confirmed that the gall mite triggered a stronger defence response than the psyllid, and the psyllid mainly affected primary metabolism but had a weaker effect on secondary metabolism. However, the results for the three phenolic compounds showed that *B. gobica* could induce the accumulation of some secondary metabolites. The ferulic acid content increased mostly in mite-infested leaves, the scoparone content increased mostly in psyllid-infested leaves, but both mites and psyllids dramatically promoted the accumulation of scopoletin. Ferulic acid, scopoletin, and scoparone all exhibit insecticidal or growth inhibitory activity (Tripathi et al. 2011; Yang et al. 2017; Zhou et al. 2022), which implies that the suppressed growth of *A. pallida* by *B. gobica* may also occur through increased secondary metabolism (Li et al. 2018).

Seeman and Walter (2022) recently summarized four well-studied systems to explore the relationship between phoretic mites and their carriers, including the mite–fungus community of scolytine bark beetles, hummingbird–flower mites, microporous–carrion beetles, and acarinarina mites–bees. Studies on all of these systems have focused on the process of phoresy. We can easily conclude that phoresy is underrepresented in the literature due to the relative difficulty of studying these systems. However, in this study, we have provided a new system to explore the interspecific interactions between phoretic mites and their vectors based on host plants after the detachment stage. Although there was no direct contact between the phoretic mite and its vector, they influenced each other via the host plant and then maintained a relatively stable ecological relationship, mitigating the leaf abscission caused by psyllid, which promoted the persistence of the psyllid population and then indirectly contributed to the phoretic association (Li et al. 2018).

Both phoretic mite–insect and gall-inducing arthropod–plant interactions are suitable systems for the study of coevolutionary relationships (Chen et al. 2020; Bartlow and Agosta 2021). We speculate that the evolutionary and ecological significance of phoresy and gall induction in gall mites is crucial; the former determines whether the gall mite survives, and the latter determines whether gall mite infestation is promoted. The results clearly showed that the gall mite *A. pallida* was not only a superior phoront carried by the psyllid *B. gobica* during overwintering but also a wise gall maker that influenced *B. gobica* by manipulating the host plant in the non-overwintering period.

Authors' contributions Mengke Yang and Jianling Li performed research, Mengke Yang analysed data and wrote the main manuscript text, Haili Qiao and Kun Guo contributed the idea of data analysis, Rong Xu and Hongshuang Wei provided suggestions for discussion organization, Jianhe Wei provided ideas for abstract writing, Sai Liu and Changqing Xu designed research, Sai Liu revised the manuscript, contributed new analytic tools and drew the integrated analysis of transcriptomic and metabolic figures, Changqing Xu provided help in the manuscript polishing. All authors read and approved the final manuscript.

Funding This research was supported by the National Key Research and Development Program of China (grant number: 2022YFC3501502), National Natural Science Foundation of China (grant number: 81673699) and Chinese Academy of Medical Sciences Innovation Fund for Medical Science (grant number: 2021-I2M-1-031).

Declarations

Conflict of interest The authors declare that they have no known competing financial interests or other personal relationships that might be perceived to influence the work reported in this paper.

References

- Addicott FT, Lynch RS (1955) Physiology of abscission. *Annu Rev Plant Physiol* 6:211–238. <https://doi.org/10.1146/annurev.pp.06.060155.001235>
- Awmack CS, Leather SR (2002) Host plant quality and fecundity in herbivorous insects. *Annu Rev Entomol* 47:817–844. <https://doi.org/10.1146/annurev.ento.47.091201.145300>
- Bartlow AW, Agosta SJ (2021) Phoresy in animals: review and synthesis of a common but understudied mode of dispersal. *Biol Rev* 96:223–246. <https://doi.org/10.1111/brv.12654>
- Behura BK (1956) The relationships of the Tyroglyphoid mite, *Histiostoma polypori* (Oud.) with the earwig, *Forficula auricularia* Linn. *J N Y Entomol Soc* 64:85–94. <https://doi.org/10.2307/25005599>
- Binns ES (1982) Phoresy as migration—some functional aspects of phoresy in mites. *Biol Rev* 57:571–620. <https://doi.org/10.1111/j.1469-185X.1982.tb00374.x>
- Byrne DN, Miller WB (1990) Carbohydrate and amino acid composition of phloem sap and honeydew produced by *Bemisia tabaci*. *J Insect Physiol* 36:433–439. [https://doi.org/10.1016/0022-1910\(90\)90061-j](https://doi.org/10.1016/0022-1910(90)90061-j)
- Chen H, Liu J, Cui K, Lu Q, Wang C, Wu HX, Yang ZX, Ding WF, Shao SX, Wang HY, Ling XF, King-Jones K, Chen XM (2018) Molecular mechanisms of tannin accumulation in *Rhus* galls and genes involved in plant-insect interactions. *Sci Rep* 8:9841–9852. <https://doi.org/10.1038/s41598-018-28153-y>
- Chen XM, Yang ZX, Chen H, Qian Q, Liu J, Wang C, Shao SX, Lu Q, Li Y, Wu HX, Jones KK, Chen MS (2020) A complex nutrient exchange between a gall-forming aphid and its plant host. *Front Plant Sci* 11:811–855. <https://doi.org/10.3389/fpls.2020.00811>
- Cheynier V, Comte G, Davies KM, Lattanzio V, Martens S (2013) Plant phenolics: recent advances on their biosynthesis, genetics, and ecophysiology. *Plant Physiol Biochem* 72:1–20. <https://doi.org/10.1016/j.plaphy.2013.05.009>
- Chin E, Godfrey K, Polek M, Slupsky C (2017) ¹H NMR analysis of *Citrus macrophylla* subjected to Asian citrus psyllid (*Diaphorina citri* Kuwayama) feeding. *Arthropod-Plant Inte* 11:901–909. <https://doi.org/10.1007/s11829-017-9546-0>
- Coelho Kuster V, Costa Rezende U, Fernandes Cardoso JC, dos Santos Isaias RM, Coelho de Oliveira D (2020) How galling organisms manipulate the secondary metabolites in the host plant tissues? A histochemical overview in neotropical gall systems. In: Mérillon JM, Ramawat KG (eds) Co-evolution of secondary metabolites. Springer, Cham, pp 823–842
- de Hoon MJ, Imoto S, Nolan J, Miyano S (2004) Open source clustering software. *Bioinformatics* 20:1453–1454. <https://doi.org/10.1093/bioinformatics/bth078>
- de Lillo E, Pozzebon A, Valenzano D, Duso C (2018) An intimate relationship between Eriophyoid mites and their host plants - a review. *Front Plant Sci* 9:1786–1799. <https://doi.org/10.3389/fpls.2018.01786>
- Dorchin N, Cramer MD, Hoffmann JH (2006) Photosynthesis and sink activity of wasp-induced galls in *Acacia pycnantha*. *Ecology* 87:1781–1791. [https://doi.org/10.1890/0012-9658\(2006\)87\[1781:pasaow\]2.0.co;2](https://doi.org/10.1890/0012-9658(2006)87[1781:pasaow]2.0.co;2)
- Eisen MB, Spellman PT, Brown PO, Botstein D (1998) Cluster analysis and display of genome-wide expression patterns. *Proc Natl Acad Sci USA* 95:14863–14868. <https://doi.org/10.1073/pnas.95.25.14863>
- Fay PA, Hartnett DC, Knapp AK (1993) Increased photosynthesis and water potentials in *Silphium integrifolium* galled by cynipid wasps. *Oecologia* 93:114–120. <https://doi.org/10.1007/BF00321200>
- Florentine SK, Raman A, Dhileepan K (2005) Effects of gall induction by *Epiblema strenuana* on gas exchange, nutrients, and energetics in *Parthenium hysterophorus*. *Biocontrol* 50:787–801. <https://doi.org/10.1007/s10526-004-5525-3>
- Fürstenberg-Hägg J, Zagrobelny M, Bak S (2013) Plant defense against insect herbivores. *Int J Mol Sci* 14:10242–10297. <https://doi.org/10.3390/ijms140510242>

- Gao F, Zhao ZH, John J, Liu TX (2016) Impact of potato psyllid density and timing of infestation on zebra chip disease expression in potato plants. *Plant Prot Sci* 52:262–269. <https://doi.org/10.17221/186/2015-pps>
- Gerchman Y, Inbar M (2011) Distinct antimicrobial activities in aphid galls on *Pistacia atlantica*. *Plant Signal Behav* 6:2008–2012. <https://doi.org/10.4161/psb.6.12.18031>
- Haiden SA, Hoffmann JH, Cramer MD (2012) Benefits of photosynthesis for insects in galls. *Oecologia* 170:987–997. <https://doi.org/10.1007/s00442-012-2365-1>
- Harrison K, Mendoza-Herrera A, Levy JG, Tamborindeguy C (2021) Lasting consequences of psyllid (*Bactericera cockerelli* L.) infestation on tomato defense, gene expression, and growth. *BMC Plant Biol* 21:114–156. <https://doi.org/10.1186/s12870-021-02876-z>
- Hijaz F, Lu Z, Killiny N (2016) Effect of host-plant and infection with ‘*Candidatus Liberibacter asiaticus*’ on honeydew chemical composition of the Asian citrus psyllid, *Diaphorina citri*. *Entomol Exp Appl* 158:34–43. <https://doi.org/10.1111/eea.12377>
- Hirano T, Kimura S, Sakamoto T, Okamoto A, Nakayama T, Matsuura T, Ikeda Y, Takeda S, Suzuki Y, Ohshima I, Sato MH (2020) Reprogramming of the developmental program of *Rhus javanica* during initial stage of gall induction by *Schlechtendalia chinensis*. *Front Plant Sci* 11:471. <https://doi.org/10.3389/fpls.2020.00471>
- Inbar M, Wink M, Wool D (2004) The evolution of host plant manipulation by insects: molecular and ecological evidence from gall-forming aphids on *Pistacia*. *Mol Phylogenet Evol* 32:504–511. <https://doi.org/10.1016/j.ympev.2004.01.006>
- Javadi Khederi S, Khanjani M, Gholami M, Panzarino O, de Lillo E (2018) Influence of the erineum strain of *Colomerus vitis* (Acari: Eriophyidae) on grape (*Vitis vinifera*) defense mechanisms. *Exp Appl Acarol* 75:1–24. <https://doi.org/10.1007/s10493-018-0252-0>
- Kaplan I, Denno RF (2007) Interspecific interactions in phytophagous insects revisited: a quantitative assessment of competition theory. *Ecol Lett* 10:977–994. <https://doi.org/10.1111/j.1461-0248.2007.01093.x>
- Kessler A, Baldwin IT (2004) Herbivore-induced plant vaccination. Part I. The orchestration of plant defenses in nature and their fitness consequences in the wild tobacco *Nicotiana attenuata*. *Plant J* 38:639–649. <https://doi.org/10.1111/j.1365-313X.2004.02076.x>
- Kot I, Jakubczyk A, Karas M, Zlotek U (2018) Biochemical responses induced in galls of three Cynipidae species in oak trees. *Bull Entomol Res* 108:494–500. <https://doi.org/10.1017/S0007485317001055>
- Larson KC, Whitham TG (1991) Manipulation of food resources by a gall-forming aphid: the physiology of sink-source interactions. *Oecologia* 88:15–21. <https://doi.org/10.1007/BF00328398>
- Lee G, Joo Y, Kim SG, Baldwin IT (2017) What happens in the pith stays in the pith: tissue-localized defense responses facilitate chemical niche differentiation between two spatially separated herbivores. *Plant J* 92:414–425. <https://doi.org/10.1111/tpj.13663>
- Li XQ, Liu YZ, Guo WF, Solanki MK, Yang ZD, Xiang Y, Ma ZC, Wen YG (2017) The gall wasp *Leptocybe invasa* (Hymenoptera: Eulophidae) stimulates different chemical and phytohormone responses in two *Eucalyptus* varieties that vary in susceptibility to galling. *Tree Physiol* 37:1208–1217. <https://doi.org/10.1093/treephys/tpx098>
- Li JL, Liu S, Guo K, Zhang F, Qiao HL, Chen JM, Yang MK, Zhu X, Xu R, Xu CQ, Chen J (2018) Plant-mediated competition facilitates a phoretic association between a gall mite and a psyllid vector. *Exp Appl Acarol* 76:325–337. <https://doi.org/10.1007/s10493-018-0315-2>
- Liu S, Li JL, Guo K, Qiao HL, Xu R, Chen JM, Xu CQ, Chen J (2016) Seasonal phoresy as an overwintering strategy of a phytophagous mite. *Sci Rep* 6:25483–25490. <https://doi.org/10.1038/srep25483>
- Liu S, Li JL, Yang MK, Qiao HL, Guo K, Xu R, Xu CQ, Chen J (2020) Influence of *Bactericera gobica* Loginova on growth of *Lycium barbarum* L. *Mod Chin Med* 22:715–710. <https://doi.org/10.13313/j.issn.1673-4890.20200229002>(in Chinese with English abstract)
- Malka O, Easson M, Paetz C, Gotz M, Reichelt M, Stein B, Luck K, Stanisic A, Juravel K, Santos-Garcia D, Mondaca LL, Springate S, Colvin J, Winter S, Gershenzon J, Morin S, Vassao DG (2020) Glucosylation prevents plant defense activation in phloem-feeding insects. *Nat Chem Biol* 16:1420–1426. <https://doi.org/10.1038/s41589-020-00658-6>
- Mattson WJ (1980) Herbivory in relation to plant nitrogen content. *Annu Rev Entomol* 11:119–161. <https://doi.org/10.1146/annurev.es.11.110180.001003>
- Meunier CL, Gundale MJ, Sanchez IS, Liess A (2016) Impact of nitrogen deposition on forest and lake food webs in nitrogen-limited environments. *Glob Change Biol* 22:164–179. <https://doi.org/10.1111/gcb.12967>
- Mitchell C, Brennan RM, Graham J, Karley AJ (2016) Plant defense against herbivorous pests: exploiting resistance and tolerance traits for sustainable crop protection. *Front Plant Sci* 7:1132–1139. <https://doi.org/10.3389/fpls.2016.01132>
- Morath S, Pratt P, Silvers C, Center T (2006) Herbivory by *Boreioglycaspis melaleucae* (Hemiptera: Psyllidae) accelerates foliar senescence and abscission in the invasive tree *Melaleuca quinquenervia*. *Environ Entomol* 35:1372–1378. <https://doi.org/10.1093/ee/35.5.1372>

- Murakami R, Ushima R, Sugimoto R, Tamaoki D, Karahara I, Hanba Y, Wakasugi T, Tsuchida T (2021) A new galling insect model enhances photosynthetic activity in an obligate holoparasitic plant. *Sci Rep* 11:13013. <https://doi.org/10.1038/s41598-021-92417-3>
- Mutwakil MZ, Hajrah NH, Atef A, Edris S, Sabir MJ, Al-Ghamdi AK, Sabir M, Nelson C, Makki RM, Ali HM, El-Domyati FM, Al-Hajar ASM, Gloaguen Y, Al-Zahrani HS, Sabir JSM, Jansen RK, Bahieldin A, Hall N (2017) Transcriptomic and metabolic responses of *Calotropis procera* to salt and drought stress. *BMC Plant Biol* 17:231–241. <https://doi.org/10.1186/s12870-017-1155-7>
- Nabity PD, Haus MJ, Berenbaum MR, DeLucia EH (2013) Leaf-galling phylloxera on grapes reprograms host metabolism and morphology. *Proc Natl Acad Sci USA* 110:16663–16668. <https://doi.org/10.1073/pnas.1220219110>
- Nakamura M, Miyamoto Y, Ohgushi T (2003) Gall initiation enhances the availability of food resources for herbivorous insects. *Funct Ecol* 17:851–857. <https://doi.org/10.1111/j.1365-2435.2003.00786.x>
- Nasareen PNM, Vardhanan YS, Ramani N (2012) Damage assessment of the gall mite *Aceria pongamiae* Keifer 1966 (Acari: Eriophyidae) on *Pongamia pinnata* (L.) Pierre. In: Sabu A, Augustine A (eds) *Prospects in Bioscience: addressing the issues*. Springer, India, pp 325–333
- Okumura E, Tanaka R, Yoshiga T (2013) Conditions for disembarkation of *Caenorhabditis japonica* from its carrier insect *Parastrachia japonensis*. *Nematol Res* 43:1–7. <https://doi.org/10.3725/jjn.43.1>
- Othmen SB, Boussaa F, Hajji-Hedfi L, Abbess K, Dbara S, Chermiti B (2022) Effects of nymphal density (*Bactericera trigonica*) and feeding on photosynthetic pigments, proline content and phenolic compounds in carrot plants. *Eur J Plant Pathol* 163:51–59. <https://doi.org/10.1007/s10658-021-02456-9>
- Patton MF, Arena GD, Salminen J-P, Steinbauer MJ, Casteel CL (2018) Transcriptome and defence response in *Eucalyptus camaldulensis* leaves to feeding by *Glycaspis brimblecombei* Moore (Hemiptera: Aphalaridae): a stealthy psyllid does not go unnoticed. *Austral Entomol* 57:247–254. <https://doi.org/10.1111/aen.12319>
- Paul MJ, Foyer CH (2001) Sink regulation of photosynthesis. *J Exp Bot* 52:1383–1400. <https://doi.org/10.1093/jexbot/52.360.1383>
- Perotti MA, Braig HR (2009) Phoretic mites associated with animal and human decomposition. *Exp Appl Acarol* 49:85–124. <https://doi.org/10.1007/s10493-009-9280-0>
- Petanovic R, Kielkiewicz M (2010) Plant-eriophyoid mite interactions: cellular biochemistry and metabolic responses induced in mite-injured plants. Part I *Exp Appl Acarol* 51:61–80. <https://doi.org/10.1007/s10493-010-9351-2>
- Prior KM, Hellmann JJ (2010) Impact of an invasive oak gall wasp on a native butterfly: a test of plant-mediated competition. *Ecology* 91:3284–3293. <https://doi.org/10.1890/09-1314.1>
- Rehill BJ, Schultz JC (2012) *Hormaphis hamamelidis* fundatrices benefit by manipulating phenolic metabolism of their host. *J Chem Ecol* 38:496–498. <https://doi.org/10.1007/s10886-012-0115-9>
- Rostas M, Maag D, Ikegami M, Inbar M (2013) Gall volatiles defend aphids against a browsing mammal. *BMC Evol Biol* 13:193. <https://doi.org/10.1186/1471-2148-13-193>
- Sarangi P, Biswas H, Gupta SK, Saha GK (2010) Mites associated with insects of agri-horticultural importance. *Proc Zool Soc* 63:67–71. <https://doi.org/10.1007/s12595-010-0009-1>
- Seeman OD, Walter DE (2022) Phoresy and mites: more than just a free ride. *Annu Rev Entomol* 21:13–22. <https://doi.org/10.1146/annurev-ento-120220-013329>
- Skoracka A, Smith L, Oldfield G, Cristofaro M, Amrine JW (2009) Host-plant specificity and specialization in eriophyoid mites and their importance for the use of eriophyoid mites as biocontrol agents of weeds. In: Ueckermann EA (ed) *Eriophyoid mites: Progress and Prognoses*. Springer, Dordrecht, pp 93–113
- Steinbauer MJ, Burns AE, Hall A, Riegler M, Taylor GS (2014) Nutritional enhancement of leaves by a psyllid through senescence-like processes: insect manipulation or plant defence? *Oecologia* 176:1061–1074. <https://doi.org/10.1007/s00442-014-3087-3>
- Stone GN, Schönrogge K (2003) The adaptive significance of insect gall morphology. *Trends Ecol Evol* 18:512–522. [https://doi.org/10.1016/s0169-5347\(03\)00247-7](https://doi.org/10.1016/s0169-5347(03)00247-7)
- Tripathi AK, Bhakuni RS, Upadhyay S, Gaur R (2011) Insect feeding deterrent and growth inhibitory activities of scopoletin isolated from *Artemisia annua* against *Spilarctia obliqua* (Lepidoptera: Noctuidae). *Insect Sci* 18:189–194. <https://doi.org/10.1111/j.1744-7917.2010.01350.x>
- Walling LL (2000) The myriad plant responses to herbivores. *J Plant Growth Regul* 19:195–216. <https://doi.org/10.1007/s0034400000026>
- Wang XW, Li P, Liu SS (2017) Whetfly interactions with plants. *Curr Opin Insect Sci* 19:70–75. <https://doi.org/10.1016/j.cois.2017.02.001>
- War AR, Paulraj MG, Ahmad T, Buhroo AA, Hussain B, Ignacimuthu S, Sharma HC (2012) Mechanisms of plant defense against insect herbivores. *Plant Signal Behav* 7:1306–1320. <https://doi.org/10.4161/psb.21663>
- White T (2015) Senescence-feeders: a new trophic sub-guild of insect herbivores. *J Appl Entomol* 139:11–22. <https://doi.org/10.1111/jen.12147>

- White PS, Morran L, de Roode J (2017) Phoresy. *Curr Biol* 27:R578–R580. <https://doi.org/10.1016/j.cub.2017.03.073>
- Wu QJ, Hou WJ, Li F, Xu BY, Xie W, Wang SL, Zhang YJ (2014) Intra- and interspecific competition between western flower thrips and sweetpotato whitefly. *J Insect Sci* 14:187. <https://doi.org/10.1093/jisesa/iecu049>
- Wu P, Ge Y, He J, Haseeb M, Zhang R (2022) Positive interactions between *Aceria pallida* and *Bactericera gobica* on Goji berry plants. *Insects* 13(7):577. <https://doi.org/10.3390/insects13070577>
- Yang J, Sun XQ, Yan SY, Pan WJ, Zhang MX, Cai QN (2017) Interaction of ferulic acid with glutathione S-transferase and carboxylesterase genes in the brown planthopper, *Nilaparvata lugens*. *J Chem Ecol* 43:693–702. <https://doi.org/10.1007/s10886-017-0859-3>
- Yang MK, Li HL, Qiao HL, Guo K, Xu R, Wei HS, Wei JH, Liu S, Xu CQ (2023) Integrated transcriptome and metabolome dynamic analysis of galls induced by the gall mite *Aceria pallida* on *Lycium barbarum* reveals the molecular mechanism underlying gall formation and development. *Int J Mol Sci* 24:9839. <https://doi.org/10.3390/ijms24129839>
- Zhou H, Wan F, Guo F, Liu J, Ding W (2022) High value-added application of a renewable bioresource as acaricide: investigation the mechanism of action of scoparone against *Tetranychus cinnabarinus*. *J Adv Res* 38:29–39. <https://doi.org/10.1016/j.jare.2021.08.013>

Publisher's Note Springer Nature remains neutral with regard to jurisdictional claims in published maps and institutional affiliations.

Springer Nature or its licensor (e.g. a society or other partner) holds exclusive rights to this article under a publishing agreement with the author(s) or other rightsholder(s); author self-archiving of the accepted manuscript version of this article is solely governed by the terms of such publishing agreement and applicable law.

Authors and Affiliations

Mengke Yang¹ · Jianling Li^{1,2} · Haili Qiao¹ · Kun Guo¹ · Rong Xu¹ · Hongshuang Wei¹ · Jianhe Wei¹ · Sai Liu¹ · Changqing Xu¹

✉ Sai Liu
sliu@implad.ac.cn

✉ Changqing Xu
cqxu@hotmail.com

¹ Institute of Medicinal Plant Development, Chinese Academy of Medical Sciences and Peking Union Medical College, No. 151 Malianwa North Road, Haidian District, Beijing 100193, China

² Qinghai Academy of Agriculture and Forestry Sciences, 253 Ningda Road, Chengbei District, Xining, Qinghai Province 810016, China